

CHAPTER 4

Insight into electronic behavior and stability criteria of Bi, BiAs and BiSb monolayers

4.1 Introduction

The discovery of graphene led successful synthesis and prediction of several 2D materials such as hexagonal boron nitride (h-BN), silicene, transition metal disulfides, phosphorene, alkali-earth metal hydroxides etc.^{6–15} Among these 2D materials, the rediscovery of black phosphorus (BP) i.e. phosphorene obtained through exfoliation from its layered bulk counterparts of group VA, monolayer and multilayer arsenic (As) and antimony (Sb) have received great attention due to their peculiar thermal, optical and electronic properties.^{11,16–21} The phosphorene exhibits buckled hexagonal structure as most stable structure and has allotropes such as symmetric-washboard (sw) and antisymmetric-washboard (aw) structured phosphorene.²² The Group VA monolayers are energetically stable in buckled hexagonal phase. The phosphorene and arsenene monolayers are also found stable in sw structure.²² The sw-phosphorene is obtained by exfoliation from bulk orthorhombic phase whereas antimonene and bismuthene are found to be stable in antisymmetric-washboard (aw) structure.²³ The Group V monolayers received lot of attention in the recent time due to their strain tuned properties such as direct-indirect band gap transition,^{17,24–27} negative Poisson's ratio,^{28,29} and topological transitions.^{30–33} Therefore, the identification of 2D semiconductors with distinct bandgap energies is of utmost importance for their specific applications. It is found that the strain or substrate modified group-V monolayers are very useful for the practical applications.³⁴ Active research has been carried out on semimetal to semi-conductor and semi-conductor to topological transitions under strain.^{14,35}

CHAPTER 4

Insight into electronic behavior and stability criteria of Bi, BiAs and BiSb monolayers

Bismuth (Bi) is the last and heaviest element of group V elements. Bi-based 2D materials are one of the best candidates for 2D topological insulator due to strong spin-orbit coupling.^{36–39} Subsequently, many studies have been carried out on 2D bismuth or bismuthene including discovery of Rashba-type spin splitting arising from the strong spin orbit coupling (SOC) and film thickness dependent surface states.^{14,34,35,40,41} In addition, the interfacial characteristics of bismuthene metal contacts have been explored in depth in which the bismuthene on the metal layer is metallized and show ohmic contact in the vertical direction.⁴² However, the effect of strain induced by the metal substrate on Bi monolayer was not considered to be of utmost importance. The shift in band edge of bismuthene due to strain alters the choice of metal electrodes in monolayer bismuthene devices. The strain dependent electronic properties of Bi, BiAs and BiSb have been previously studied, however, the stability of free-standing BiAs and BiSb monolayers is questionable under strain.^{35,40} This suggests that the lattice dynamical properties of these materials under strain need further attention. The systematic study of strain dependent lattice dynamics and elastic constants provides a deeper understanding of its dynamical and mechanical stabilities.

In the present chapter, we report results on the systematically investigated electronic, optical, mechanical and lattice dynamical properties of two-dimensional bismuth (Bi), bismuth arsenide (BiAs) and bismuth antimonide (BiSb). The objective is to understand the modification of electronic band structure of 2D Bi, BiAs and BiSb with compressive and tensile strains and to find their stability limit under applied strain.

CHAPTER 4

Insight into electronic behavior and stability criteria of Bi, BiAs and BiSb monolayers

4.2 Computational methods

All calculations in the present study were performed using density functional theory based first principles calculations with a plane wave pseudopotential method as implemented in Quantum Espresso code.⁴³ The Generalized gradient approximation (GGA) was used for exchange correlation functional in which the energy was parameterized by Perdew–Burke–Ernzerhof (PBE).^{44,45} The energy cut-off values for charge density and plane wave basis set for single particle wave functions were 80 Ry and 800 Ry respectively, which were sufficient to fully converge the lattice parameters and total energy. We used 16 x 16 x 1 **k**-point grids for the unit cell in the Monkhorst-Pack scheme.⁴⁶ The calculation of phonon frequencies using the perturbation method⁴⁷ along the full Brillouin Zone (BZ) is an assurance of dynamical stability. We have applied acoustic sum rule for $q \rightarrow 0$ and calculated dynamical matrix for 2D monolayer of Bi, BiAs and BiSb using 4 x 4 x 1 **q**-mesh. The elastic constants C_{ij} were calculated using the stress-strain relationship as implemented in the Elastic Code. Elastic constants were converged better than 1GPa by increasing the k -mesh size. The bulk modulus (B), shear modulus (G), Young's modulus (E) and Poisson's ratio (ν) were first determined using the Voigt and Reuss bounds schemes and then an arithmetic average was computed following the Voigt-Reuss-Hill averaging scheme.^{48–50} This way of evaluating elastic moduli is important since the Voigt and Reuss bounds respectively give an upper and lower estimate of the actual elastic moduli of polycrystalline crystals. The Voigt bound scheme relies on the assumption of uniform strain throughout the crystal, whereas the Reuss bound scheme relies on the assumption of uniform stress throughout the crystal. After successful prediction of the bandgap and electronic

CHAPTER 4

Insight into electronic behavior and stability criteria of Bi, BiAs and BiSb monolayers

properties, we calculated optical properties with random phase approximation (RPA) using the long wavelength expression for imaginary part of the dielectric tensor. The real part of the dielectric tensor is determined using the Krammers-Kroning relation.⁵¹ After acquiring the dielectric function, we have calculated the absorption coefficient $\alpha = \frac{4\pi E}{hc} \widehat{K}(E)$ where h and c are Planck's constant and speed of light respectively. Here $\widehat{K}(E) = \sqrt{(\varepsilon_r(\omega)^2 + \varepsilon_i(\omega)^2) - \varepsilon_r(\omega)}$; ε_r and ε_i are real and imaginary part of dielectric constant respectively.

4.3 Results and discussion

4.3.1 Structural and electronic properties

The elementary group-V monolayers have several stable isomeric phases but the energetically most favorable phase is buckled hexagonal (*bh*) like silicene and germanene as shown in Fig. 4.1(a-c). In this study, we focused on the buckled hexagonal phase of bismuthene and its binary BiAs and BiSb monolayers. The bismuthene has 2D hexagonal lattice, where each atom is covalently bonded with three Bi neighboring atoms. The lattice constant and buckling height (Δh) are listed in Table 4.1. The buckling height Δh is 1.72 Å while bond length is 3.04 Å. The planar sp^2 bonding is dehybridized to compensate weak π - π bonding like graphene to form sp^3 hybridization.⁴ The BiAs and BiSb monolayers exhibit similar structure, where three Bi atoms are covalently bonded with corresponding neighboring As and Sb atoms respectively

CHAPTER 4

Insight into electronic behavior and stability criteria of Bi, BiAs and BiSb monolayers

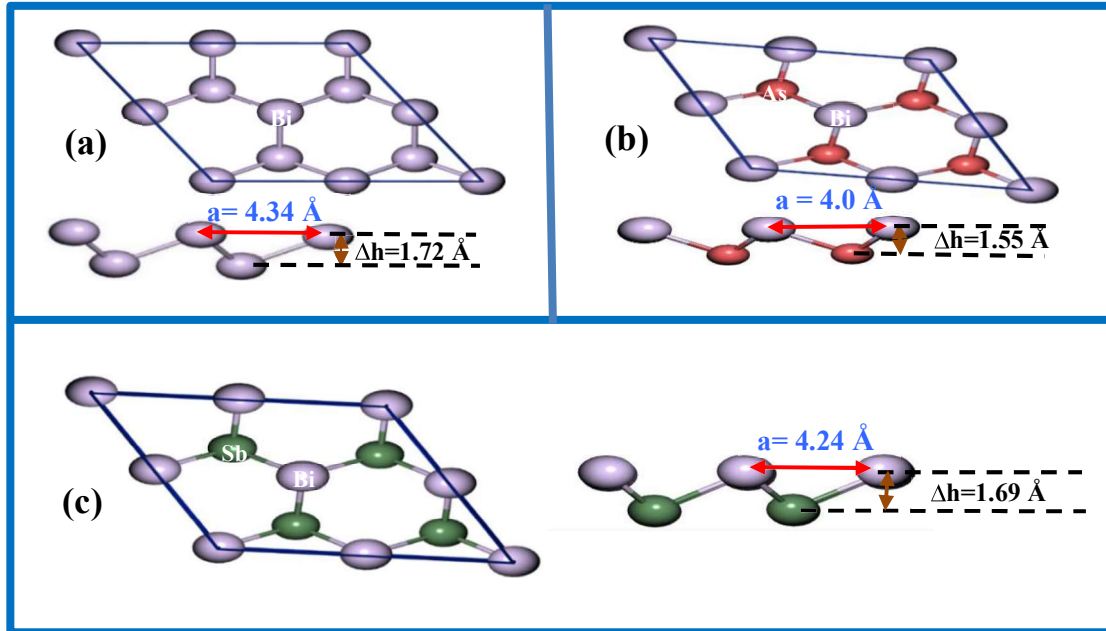


Figure 4.1: (a) Top and side view of optimized structure of monolayer buckled hexagonal (hb) (a) bismuthine (b) bismuth arsenide and bismuth antimonide. Purple, red and green balls represent bismuth, arsenic and antimony atoms respectively.

or vice-versa. Since atoms are switched with As and Sb, the buckling height and bond angles also change to overcome the steric effect. The lattice constants and buckling heights are in good

Table 4.1: Calculated Lattice constant 'a' (Å), Bond length (Å), Buckling height(Å), Energy band gap E_g (eV) and Fermi level energies E_F (eV) of 2D Bi, BiAs and BiSb monolayers.

System	Lattice constant (Å)	Δh (Å)	Bond length (Å)	E_F (eV)	E_g (eV)
Bi	4.34, 4.3-4.45 ^{22,35,41}	1.72, 1.74 ³⁵	3.04, 3.05 ³⁵	-1.44	0.61
BiAs	4.0, 3.99 ³⁵	1.54, 1.55 ³⁵	2.78, 2.78 ³⁵	-1.88	1.11
BiSb	4.24, 4.22 ³⁵	1.68, 1.69 ³⁵	2.97, 2.97 ³⁵	-1.63	0.99

CHAPTER 4

Insight into electronic behavior and stability criteria of Bi, BiAs and BiSb monolayers

agreement with previously reported data.^{22,35,41} The calculated electronic band structure of Bi, BiAs and BiSb monolayers is presented in Fig. 4.2(a-c) which depicts that the 2D Bi, BiAs and

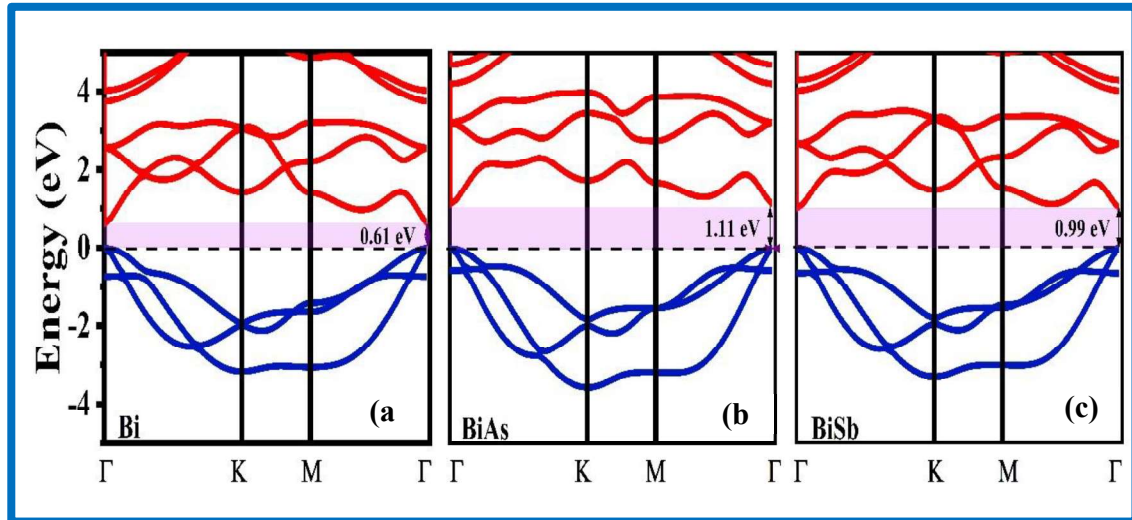


Figure 4.2: Electronic band structure of 2D monolayer (a) Bi, (b) BiAs and (c) BiSb.

BiSb exhibit direct bandgap semi-conducting nature with band gap value of 0.66 eV, 1.11 eV and 0.97 eV respectively. We observe that the band-gap of BiAs and BiSb is larger compared to Bi suggesting its versatility and potential applications in opto-electronic, photocatalyst and solar cell. The direct bandgap occurs at Γ point of the BZ as the conduction band minima (CBM) and valence band maxima (VBM) is located at this point. In addition, there is no significant change in the band dispersion for valence band except the opening and closing of upper band set at **K** and **M** points of the BZ respectively.

4.3.1.1 Optical properties

Analysis of optical properties of materials is an important factor for opto-electronic device fabrication. As Bi, BiAs and BiSb exhibit smaller band gap around 1 eV they can be suitable materials for optoelectronic applications. We know that the wavelength is inversely

CHAPTER 4

Insight into electronic behavior and stability criteria of Bi, BiAs and BiSb monolayers

proportional to bandgap energy and photons with lower energy or longer wavelength compared to corresponding bandgap is not absorbed. Therefore, if the photon energy of an incident light is lower than the bandgap energy of a material, the material appears to be transparent for corresponding wavelength of light. The absorption coefficient of materials plays a vital role to

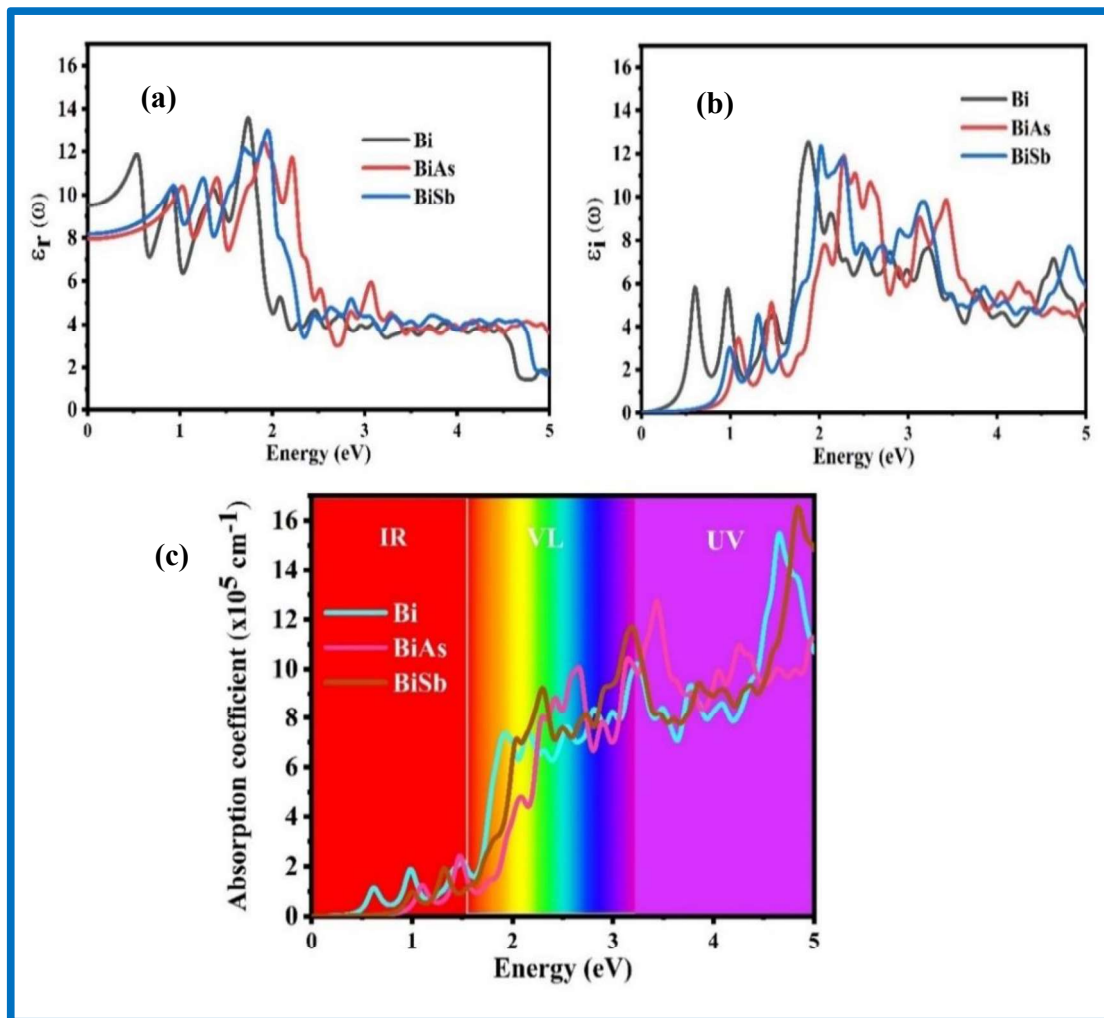


Figure 4.3: (a) Real part of dielectric constant, (b) imaginary part of dielectric constant and (c) absorption coefficient of monolayer Bi, BiAs and BiSb.

CHAPTER 4

Insight into electronic behavior and stability criteria of Bi, BiAs and BiSb monolayers

know the potential of materials to be used in photo catalyst, solar cell devices and optoelectronics. The optical absorption properties of Bi, BiAs and BiSb monolayers are studied by computing the components of dielectric functions $\epsilon_r(\omega)$ and $\epsilon_i(\omega)$, where $\epsilon_i(\omega)$ is the imaginary part related to absorption at a given frequency ω and $\epsilon_r(\omega)$ is the real part of dielectric constant. Fig. 4.3(a) clearly depicts that the dielectric function is maximum around 1.7–2.15 eV for all three monolayers. In case of BiAs and BiSb monolayers, the peak with minimum intensity for of dielectric function is around 4.8–5.0 eV suggesting transparency for high-energy incident photon and metallic nature in this region. In the case of Bi, it attains minima near 2.8 eV which indicates that the Bi monolayer exhibits metallic nature in this region. Comparing, three monolayers, Bi is less suitable for optoelectronic device applications compared to BiAs and BiSb. The imaginary part of the dielectric constants plays a significant role in the interpretation of interband-transition. Fig. 4.3(b) clearly depicts two peaks at 0.6 eV for CBM- Γ and at 1 eV at CBM ($M-\Gamma$). These show that the Bi exhibits direct band gap nature of 0.6 eV and indirect band gap of 1 eV between $M-\Gamma$ points of the BZ. Similarly, two peaks are observed for BiAs and BiSb at 1.1 eV and 0.98 eV respectively which exhibit their direct band gap nature. The absorption coefficient shown in Fig. 4.3(c) shows a blue shift going from Bi to BiSb indicating that the band gap increases as we move from Bi to BiSb. We can clearly see from the Fig. 4.3(c) that all three monolayers show considerable absorption in IR region due to small band gap. These materials show properties which are appropriate for water splitting as photocatalyst. The electronic properties including bandgap of these materials can be tuned under strain which occurs due to adhesion effect of substrate.

CHAPTER 4

Insight into electronic behavior and stability criteria of Bi, BiAs and BiSb monolayers

4.3.1.2 Electronic properties under strain

Now we will analyze strain effect on electronic properties of these monolayers. We have analyzed the evolution of the band structure with compressive and tensile strains for 2D Bi, BiAs and BiSb and presented them in Fig. 4.4(a-c). These figures represent the energy of VBM at Γ point (VBM- (Γ)), CBM at Γ (CBM- (Γ)), CBM at valley lying between Γ and M points (CBM ($M-\Gamma$)) and CBM at K point (CBM-(K)) with applied strain percentage. We found that all

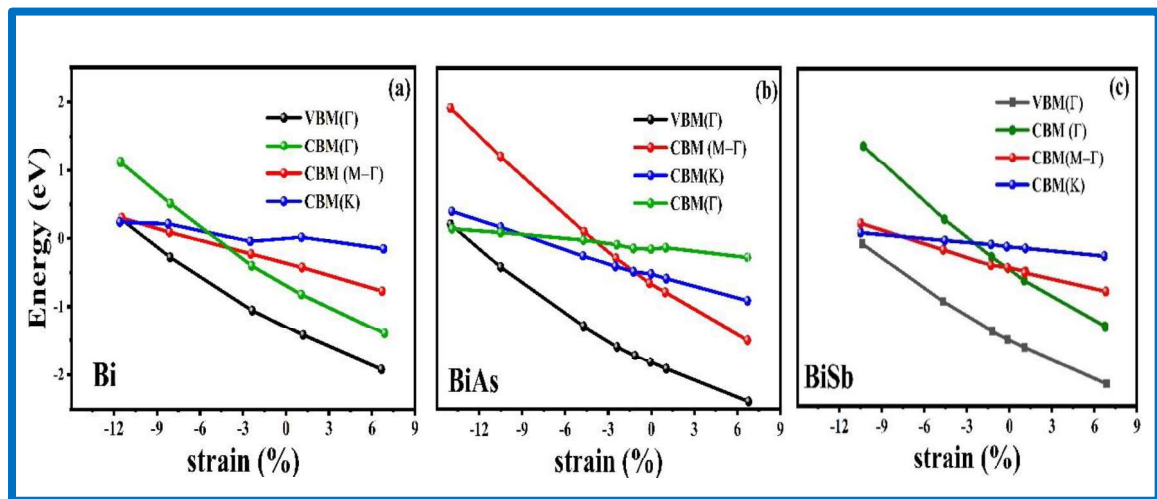


Figure 4.4: The calculated VBM, CBM at Γ , CBM at valley and CBM at K as a function of strain for (a) Bi, (b) BiAs and (c) BiSb.

monolayers preserved its direct band gap nature up to 5% of tensile strain as all curves decrease smoothly and no intersection of curve is observed. In addition, no band closing is observed up to 5% of tensile strain which shows versatility of these monolayers. It is interesting to note that the rate of decrease of CBM- Γ is faster compared to CBM at K and M points. These indicate that closing of band gap at Γ point will occur at much higher strain.

CHAPTER 4

Insight into electronic behavior and stability criteria of Bi, BiAs and BiSb monolayers

However, interesting changes are observed under compressive strain where crossover of CBM curves occurs at -5%, -3% and -2% respectively in Bi, BiAs and BiSb monolayers. This can be

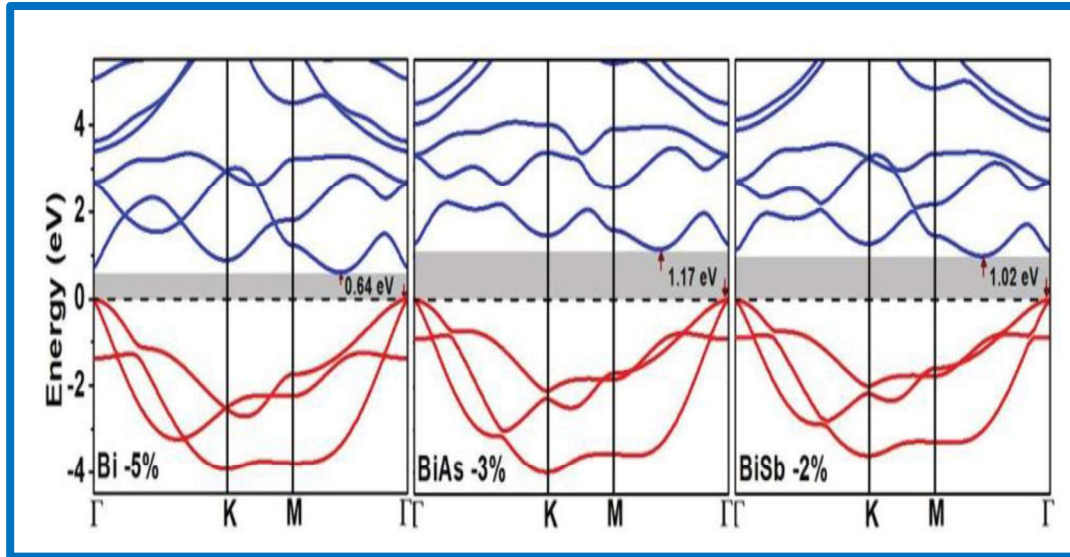


Figure 4.5: The electronic band structure of (a) Bi, (b) BiAs and (c) BiSb under compressive strain where they turn into indirect band gap semi-conductor.

attributed to the transition from direct to indirect band transition. Under compression the CBM shifts towards conduction valley in Γ - M direction. We observe indirect band gap nature in Fig. 4.5 (a-c) for Bi, BiAs and BiSb at -5%, -3% and -2% respectively. It is very crucial in determining interfacial properties of bismuthene-metal contact due to its direct to indirect transition under small amount of compressive strain for device applications.^{15,52} However, on increasing compressive strain further, the CBM shifts towards K point of the Brillouin zone. The band gap closes at higher compressive strain about -11%, -13% and -11% for Bi, BiAs and BiSb respectively. In a nutshell, all three monolayers undergo direct-indirect-metal transition under compressive strain whereas they preserve direct band gap nature under tensile strain.

CHAPTER 4

Insight into electronic behavior and stability criteria of Bi, BiAs and BiSb monolayers

4.3.2 Vibrational properties

To understand the lattice instability and vibrational characteristics such as infrared (IR) and Raman spectra, it is essential to calculate the phonon dispersion curves (PDC) of given material. In fact, phonon calculations can assist to calculate the phonon density of states which in turn help in determining the thermodynamic parameters such as Debye temperature, free energy, specific heat etc. using quasi-harmonic approximation. Furthermore, the phonons provide an insight into the mechanical, acoustical, spectroscopic and dynamical properties of

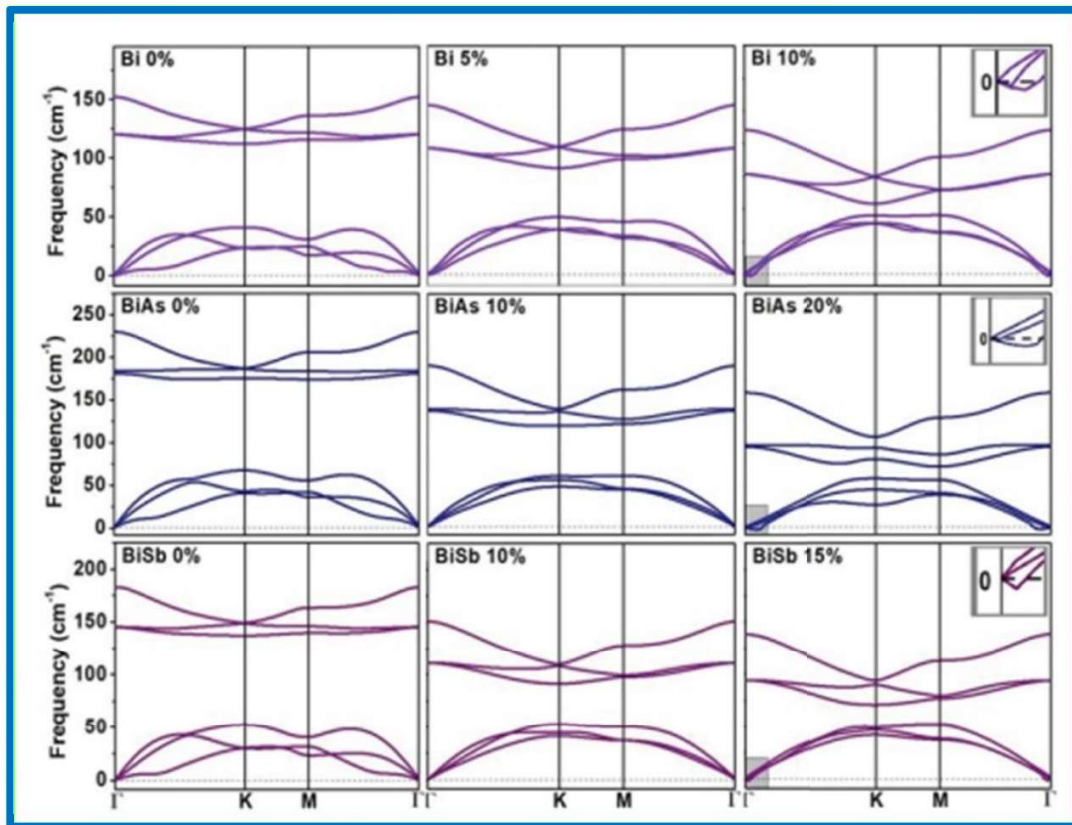


Figure 4.6: Phonon dispersion curves as a function of strain for Bi, BiAs and BiSb.

CHAPTER 4

Insight into electronic behavior and stability criteria of Bi, BiAs and BiSb monolayers

materials at finite temperature.^{53–56} The PDC which is calculated using dynamical matrix diagonalization is a true test of dynamical stability of any material.^{57–59} The calculated PDC for Bi, BiAs and BiSb monolayers along high symmetry directions of the BZ are shown in Fig. 4.6. The two atoms per unit-cell of 2D Bi, BiAs and BiSb result into total six phonon branches. The quadratic nature of the out of plane mode (ZA) arises due to the out of plane vibrations. These can be endorsed to the lowest-order amplitude and strain energy induced by this vibration together with the arching of this out-of-plane bending mode. Absence of imaginary frequencies in PDC confirms the dynamical stability of Bi, BiAs and BiSb monolayers. Similar features are observed in other 2D materials such as graphene, MoS₂ and BN layers.^{12,60,61} After observing, the strain effect over electronic properties of these 2D materials, we analyzed strain dependence of PDC of Bi, BiAs and BiSb monolayers. These analyses provide the information regarding elastic limit of monolayers beyond which they tend to lose their stability. We observe that the ZA mode is more sensitive towards biaxial strain as it turns to linear from its characteristic quadratic nature. This transformation of quadratic to linear nature is due to the removal of rippling in these monolayers as observed in case of BN sheet.⁶¹ The existing gap between optical and acoustical phonon modes at zero strain of these monolayers reduces with strain. The rate of decrease in the frequency of the modes of any materials depends on the strain created by the adhesion of these materials with substrate. Further, we observed that the Bi, BiAs and BiSb monolayers become dynamically unstable at 10%, 20% and 15 % strain respectively. Thus, the BiAs and BiSb monolayers can withstand more strain than the Bi monolayer and indicates their suitability for semi-conductor device applications.

CHAPTER 4

Insight into electronic behavior and stability criteria of Bi, BiAs and BiSb monolayers

4.3.3 Mechanical properties

A thorough knowledge of mechanical properties of any substance is crucial for their technological implementations along with its dynamical stability. The investigation of elastic constants play a vital role in understanding the characteristic of the materials such as hardness, mechanical strength, anisotropy and propagation of the sound and elastic waves and macroscopic response.⁶²⁻⁶⁵ The Poisson's ratio describes the proportion of the transverse contraction to the longitudinal expansion of a material during the stretching phase. Materials with a negative Poisson's ratio are known as auxetic materials and have drawn particular attention of scientists owing to their outstanding benefits in sensing technology. The auxetic materials expands in transverse direction, when it is stretched in longitudinal direction and vice versa. The second order elastic constants exhibit the linear elastic response whereas the higher (>2) order elastic constants characterize the nonlinear elastic response. We have calculated the second order elastic constants to know the linear elastic response of Bi, BiAs and BiSb monolayers. To know the mechanical stability of any material, the material has to satisfy Born stability criteria.⁶⁶ The Bi, BiAs and BiSb monolayers exhibit hexagonal structure. The Born criteria for 2D hexagonal structure are $C_{11} > 0.0$, $C_{11}-C_{12} > 0.0$ and $C_{66} > 0.0$. We found that all three monolayers are mechanically stable as they satisfy Born criteria. The obtained elastic constant values; $C_{11} = 18.9$ N/m, $C_{12} = 4.8$ N/m and $C_{66} = 8.4$ N/m of Bi monolayer are consistent with previous report.⁴¹ The elastic constants for BiAs and BiSb monolayers respectively are $C_{11} = 27.1$ and 21.8 N/m, $C_{12} = 9.3$ and 4.8 N/m and $C_{66} = 15.2$ and 8.4 N/m and found to be mechanically stable. We observe that among three monolayers, BiAs exhibits higher value of

CHAPTER 4

Insight into electronic behavior and stability criteria of Bi, BiAs and BiSb monolayers

planar elastic stiffness constants (C_{11} and C_{12}) suggesting better sustainability for BiAs against higher strain. Poisson's ratio ν is related to the uniaxial deformation with the volume change and higher Poisson's ratio tends to better plasticity of the materials. The Poisson's ratio of 2D Bi,

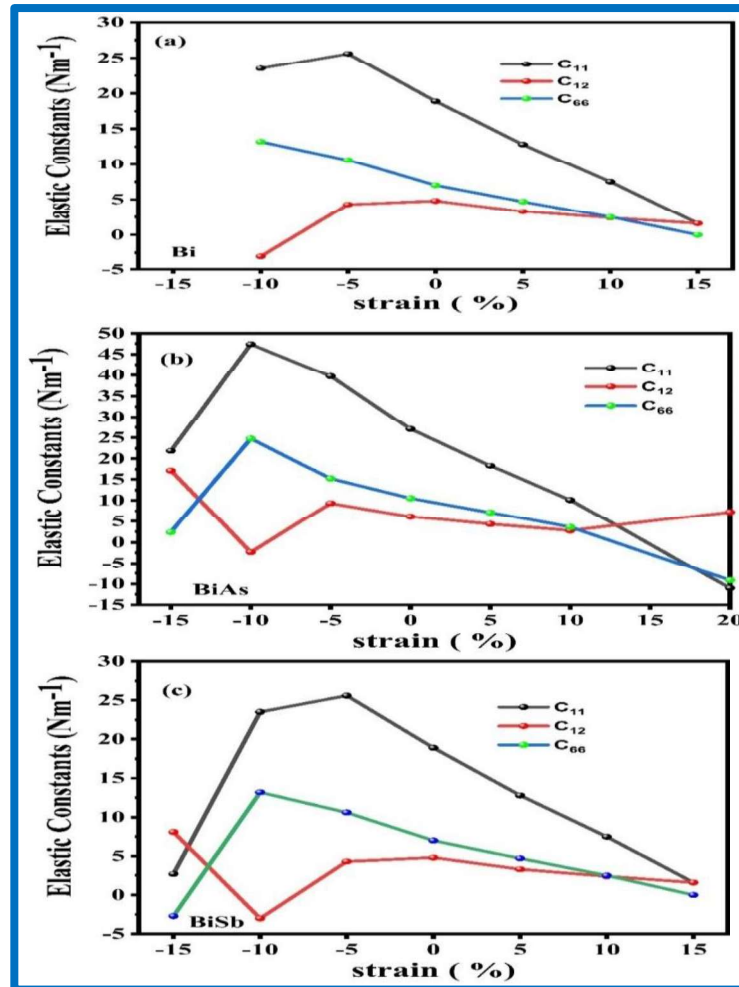


Figure 4.7: The calculated elastic constants as a function of strain for (a) Bi, (b) BiAs and (c) BiSb.

BiAs and BiSb is 0.22, 0.21 and 0.21 respectively which is very close to graphene ($\nu=0.18$) indicating covalent nature and increased brittleness.⁶⁴ Fig. 4.7 presents the elastic constants as a function of strain where it can be seen that all materials close to 15 % of tensile and

CHAPTER 4

Insight into electronic behavior and stability criteria of Bi, BiAs and BiSb monolayers

compressive strains become mechanically unstable. It is interesting to note that Bi monolayer above 10 % strain becomes dynamically unstable whereas it is mechanically unstable above 15 %.

We conclude that these monolayers are brittle at high strain and can be used in device fabrication. The bulk and shear moduli of 2D Bi, BiAs and BiSb decrease with applied compressive strain while they increase with tensile strain. The Young's modulus of 2D BiAs and BiSb increases upto -10 % compressive strains and decreases and become negative beyond

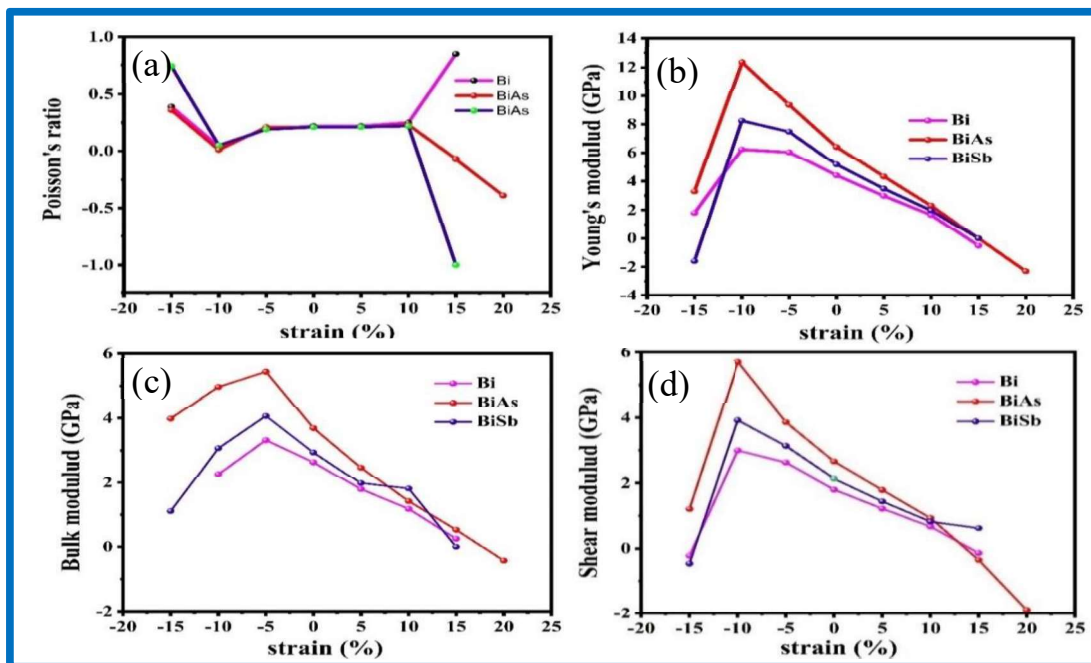


Figure 4.8: The calculated (a) Poisson's ratio (b) Young's modulus (c) Bulk modulus and (d) Shear modulus as a function of strain for Bi, BiAs and BiSb monolayers.

this (see Fig. 4.8). Thus, in our study, we observe that all these materials become mechanically unstable beyond 15 % strain. We observe that the Poisson's ratio remains constant upto 10 % of tensile strain beyond which BiAs and BiSb monolayers show auxetic behavior as Poisson's ratio becomes negative.

CHAPTER 4

Insight into electronic behavior and stability criteria of Bi, BiAs and BiSb monolayers

4.4 Conclusions

In the present work, we have carried out a systematic study of the electronic, optical, mechanical and dynamical properties of the two-dimensional Bi, BiAs and BiSb using first principles calculations based on density functional theory. We found that the monolayers of Bi, BiAs and BiSb monolayers exhibit semi-conducting nature with direct band gap of 0.66 eV, 1.11 eV and 0.99 eV respectively. The optical band gap of Bi, BiAs and BiSb monolayers is found as 0.6 eV, 1.1 eV and 0.98 eV respectively which are same as their electronic band gap. The absorption spectra show that these materials absorb radiation in IR region and hence show their use as a photocatalyst. The phonon dispersion calculations show that all three monolayers are dynamically stable as all phonon modes have real frequencies throughout the Brillouin zone. We predict that the compressive strain induces direct-indirect-metallic transition whereas tensile strain retains its direct bandgap nature. The phonon dispersion curves of these monolayers contain characteristic out-of-plane optical and acoustical phonon mode modes apart from usual longitudinal and transverse optical and acoustical mode like other 2D materials like graphene, hexagonal BN, MoS₂ etc. The out-of-plane acoustical mode which is quadratic with wave vector near zone center, turns linear under strain effect. Besides dynamical stability, these monolayers show high mechanical stability up to 15 %, 20 % and 15 % strain respectively for Bi, BiAs and BiSb. Owing to greater stability at high strain, BiAs and BiSb can be potential candidates in electronic, optoelectronic and solar cell devices.

CHAPTER 4

Insight into electronic behavior and stability criteria of Bi, BiAs and BiSb monolayers

References

- ¹ D. Pacile, J.C. Meyer, Ç.Ö. Girit, and A. Zettl, *Appl. Phys. Lett.* **92**, 133107 (2008).
- ² K.S. Novoselov, D. Jiang, F. Schedin, T.J. Booth, V. V Khotkevich, S. V Morozov, and A.K. Geim, *Proc. Natl. Acad. Sci.* **102**, 10451 (2005).
- ³ Q.H. Wang, K. Kalantar-Zadeh, A. Kis, J.N. Coleman, and M.S. Strano, *Nat. Nanotechnol.* **7**, 699 (2012).
- ⁴ S.Z. Butler, S.M. Hollen, L. Cao, Y. Cui, J.A. Gupta, H.R. Gutiérrez, T.F. Heinz, S.S. Hong, J. Huang, A.F. Ismach, and others, *ACS Nano* **7**, 2898 (2013).
- ⁵ A.K. Geim and I. V Grigorieva, *Nature* **499**, 419 (2013).
- ⁶ J. Klinovaja and D. Loss, *Phys. Rev. B* **88**, 1 (2013).
- ⁷ Y. Xu, Z. Gan, and S.-C. Zhang, *Phys. Rev. Lett.* **112**, 226801 (2014).
- ⁸ Y.-N. Xu and W.Y. Ching, *Phys. Rev. B* **44**, 7787 (1991).
- ⁹ W. Choi, N. Choudhary, G.H. Han, J. Park, D. Akinwande, and Y.H. Lee, *Mater. Today* **20**, 116 (2017).
- ¹⁰ K. Takeda and K. Shiraishi, *Phys. Rev. B* **50**, 14916 (1994).
- ¹¹ H. Liu, A.T. Neal, Z. Zhu, Z. Luo, X. Xu, D. Tománek, and P.D. Ye, *ACS Nano* **8**, 4033 (2014).
- ¹² H. Soni and P.K. Jha, *AIP Adv.* **5**, 107103 (2015).
- ¹³ K. Patel, B. Roondhe, S.D. Dabhi, and P.K. Jha, *J. Hazard. Mater.* **351**, 337 (2018).
- ¹⁴ S.B. Pillai, S. Narayan, S.D. Dabhi, and P.K. Jha, in *AIP Conf. Proc.* **1731**, 090024 (2016).
- ¹⁵ S.B. Pillai, S.D. Dabhi, S. Narayan, and P.K. Jha, in *AIP Conf. Proc.* **1942**, 90022 (2018).
- ¹⁶ Z. Luo, J. Maassen, Y. Deng, Y. Du, R.P. Garrelts, M.S. Lundstrom, D.Y. Peide, and X. Xu, *Nat. Commun.* **6**, 8572 (2015).

CHAPTER 4

Insight into electronic behavior and stability criteria of Bi, BiAs and BiSb monolayers

-
- ¹⁷ S. Zhang, Z. Yan, Y. Li, Z. Chen, and H. Zeng, *Angew. Chemie Int. Ed.* **54**, 3112 (2015).
- ¹⁸ D. Çakir, C. Sevik, and F.M. Peeters, *Phys. Rev. B* **92**, 165406 (2015).
- ¹⁹ D. Çakir, H. Sahin, and F.M. Peeters, *Phys. Rev. B* **90**, 205421 (2014).
- ²⁰ A. Chaves, T. Low, P. Avouris, D. Çakir, and F.M. Peeters, *Phys. Rev. B* **91**, 155311 (2015).
- ²¹ Z. Zhu and D. Tománek, *Phys. Rev. Lett.* **113**, 226801 (2014).
- ²² F. Ersan, D. Kecik, V.O. Özçelik, Y. Kadioglu, O.Ü. Aktürk, E. Durgun, E. Aktürk, and S. Ciraci, *Appl. Phys. Rev.* **6**, 021308 (2019).
- ²³ W. Lu, H. Nan, J. Hong, Y. Chen, C. Zhu, Z. Liang, X. Ma, Z. Ni, C. Jin, and Z. Zhang, *Nano Res.* **7**, 853 (2014).
- ²⁴ A. Manjanath, A. Samanta, T. Pandey, and A.K. Singh, *Nanotechnology* **26**, 075701 (2015).
- ²⁵ G. Wang, R. Pandey, and S.P. Karna, *ACS Appl. Mater. Interfaces* **7**, 11490 (2015).
- ²⁶ Q. Peng, A.K. Dearden, J. Crean, L. Han, S. Liu, X. Wen, and S. De, *Nanotechnol. Sci. Appl.* **7**, 1 (2014).
- ²⁷ C. Kamal and M. Ezawa, *Phys. Rev. B* **91**, 085423 (2015).
- ²⁸ J. Han, J. Xie, Z. Zhang, D. Yang, M. Si, and D. Xue, *Appl. Phys. Express* **8**, 041801(2015).
- ²⁹ J.W. Jiang and H.S. Park, *Nat. Commun.* **5**, 4727 (2014).
- ³⁰ Y. Lu, D. Zhou, G. Chang, S. Guan, W. Chen, Y. Jiang, J. Jiang, X. Sen Wang, S.A. Yang, Y.P. Feng, Y. Kawazoe, and H. Lin, *Npj Comput. Mater.* **2**, 16011 (2016).
- ³¹ P.L. Gong, D.Y. Liu, K.S. Yang, Z.J. Xiang, X.H. Chen, Z. Zeng, S.Q. Shen, and L.J. Zou, *Phys. Rev. B* **93**, 195434 (2016).
- ³² Z.J. Xiang, G.J. Ye, C. Shang, B. Lei, N.Z. Wang, K.S. Yang, D.Y. Liu, F.B. Meng, X.G. Luo, L.J. Zou, Z. Sun, Y. Zhang, and X.H. Chen, *Phys. Rev. Lett.* **115**, 186403 (2015).

CHAPTER 4

Insight into electronic behavior and stability criteria of Bi, BiAs and BiSb monolayers

-
- ³³ R. Fei, V. Tran, and L. Yang, *Phys. Rev. B* **91**, 195319 (2015).
- ³⁴ G. Giovannetti, P.A. Khomyakov, G. Brocks, P.J. Kelly, and J. Van Den Brink, *Phys. Rev. B* **76**, 73103 (2007).
- ³⁵ Y. Nie, M. Rahman, D. Wang, C. Wang, and G. Guo, *Sci. Rep.* **5**, 17980 (2015).
- ³⁶ F. Reis, G. Li, L. Dudy, M. Bauernfeind, S. Glass, W. Hanke, R. Thomale, J. Schäfer, and R. Claessen, *Science* **357**, 287 (2017).
- ³⁷ C. Sabater, D. Gosálbez-Martínez, J. Fernández-Rossier, J.G. Rodrigo, C. Untiedt, and J.J. Palacios, *Phys. Rev. Lett.* **110**, 176802 (2013).
- ³⁸ M. Wada, S. Murakami, F. Freimuth, and G. Bihlmayer, *Phys. Rev. B* **83**, 121310 (2011).
- ³⁹ F. Yang, L. Miao, Z.F. Wang, M.Y. Yao, F. Zhu, Y.R. Song, M.X. Wang, J.P. Xu, A. V. Fedorov, Z. Sun, G.B. Zhang, C. Liu, F. Liu, D. Qian, C.L. Gao, and J.F. Jia, *Phys. Rev. Lett.* **109**, 016801 (2012).
- ⁴⁰ S. Singh and A.H. Romero, *Phys. Rev. B* **95**, 165444 (2017).
- ⁴¹ E. Aktürk, O.Ü. Aktürk, and S. Ciraci, *Phys. Rev. B* **94**, 14115 (2016).
- ⁴² Y. Guo, F. Pan, M. Ye, X. Sun, Y. Wang, J. Li, X. Zhang, H. Zhang, Y. Pan, Z. Song, and others, *ACS Appl. Mater. Interfaces* **9**, 23128 (2017).
- ⁴³ P. Giannozzi, S. Baroni, N. Bonini, M. Calandra, R. Car, C. Cavazzoni, D. Ceresoli, G.L. Chiarotti, M. Cococcioni, I. Dabo, A. Dal Corso, S. De Gironcoli, S. Fabris, G. Fratesi, R. Gebauer, U. Gerstmann, C. Gougoussis, A. Kokalj, M. Lazzeri, L. Martin-Samos, N. Marzari, F. Mauri, R. Mazzarello, S. Paolini, A. Pasquarello, L. Paulatto, C. Sbraccia, S. Scandolo, G. Sclauzero, A.P. Seitsonen, A. Smogunov, P. Umari, and R.M. Wentzcovitch, *J. Phys. Condens. Matter* **21**, 395502 (2009).
- ⁴⁴ J. Perdew, K. Burke, and M. Ernzerhof, *Phys. Rev. Lett.* **77**, 3865 (1996).
- ⁴⁵ J.P. Perdew, K. Burke, and M. Ernzerhof, *Phys. Rev. Lett.* **78**, 1396 (1997).

CHAPTER 4

Insight into electronic behavior and stability criteria of Bi, BiAs and BiSb monolayers

-
- ⁴⁶ H.J. Monkhorst and J.D. Pack, Phys. Rev. B - Condens. Matter Mater. Phys. **13**, 5188 (1976).
- ⁴⁷ S. Baroni, S. De Gironcoli, A. Dal Corso, and P. Giannozzi, Rev. Mod. Phys. **73**, 515 (2001).
- ⁴⁸ W. Voigt, Lehrbuch Der Kristallphysik , Springer-Verlag (2013).
- ⁴⁹ R. Hill, Proc. Phys. Soc. Sect. A, 396 (1952).
- ⁵⁰ A. Reuss, ZAMM - J. Appl. Math. Mech. Zeitschrift Für Angew. Math. Und Mech. **9**, 49 (1929).
- ⁵¹ J. Harl, L. Schimka, and G. Kresse, Phys. Rev. B - Condens. Matter Mater. Phys. **81**, (2010).
- ⁵² M.Y. Liu, Y. Huang, Q.Y. Chen, Z.Y. Li, C. Cao, and Y. He, RSC Adv. **7**, 39546 (2017).
- ⁵³ P.K. Jha, S.D. Gupta, and S.K. Gupta, AIP Adv. **2**, 022120 (2012).
- ⁵⁴ P.K. Jha, Phys. Rev. B **72**, 214502 (2005).
- ⁵⁵ H.R. Soni and P.K. Jha, Solid State Commun. **189**, 58 (2014).
- ⁵⁶ P.K. Jha and S.P. Sanyal, Physica C: Superconductivity **261**, 259 (1996).
- ⁵⁷ P.K. Jha, Phys. Rev. B - Condens. Matter Mater. Phys. **72**, 1 (2005).
- ⁵⁸ S.D. Gupta and P.K. Jha, Earth Planet. Sci. Lett. **401**, 31 (2014).
- ⁵⁹ S.D. Gupta, S.K. Gupta, P.K. Jha, and N.N. Ovsyuk, J. Raman Spectrosc. **44**, 926-933 (2013).
- ⁶⁰ S.K. Gupta, H.R. Soni, and P.K. Jha, AIP Adv. **3**, 032117 (2013).
- ⁶¹ P.K. Jha and H.R. Soni, J. Appl. Phys. **115**, 023509 (2014).
- ⁶² G. Moynihan, S. Sanvito, and D.D. O'Regan, 2D Mater. **4**, 045018 (2017).
- ⁶³ E. Aktürk, O.Ü. Aktürk, and S. Ciraci, Phys. Rev. B **94**, 1 (2016).
- ⁶⁴ R. John and B. Merlin, Cryst. Struct. Theory Appl. **5**, 43 (2016).
- ⁶⁵ W.C. Hu, Y. Liu, D.J. Li, X.Q. Zeng, and C.S. Xu, Comput. Mater. Sci. **83**, 27-34 (2014).
- ⁶⁶ Q. Hu, Q. Wu, Y. Ma, L. Zhang, Z. Liu, J. He, H. Sun, H.T. Wang, and Y. Tian, Phys. Rev. B **73**, 1 (2006).